Rock Mechanics in the National Interest, Elsworth, Tinucci & Heasley (eds),
© 2001 Swets & Zeitlinger Lisse, ISBN 90 2651 827 7

Geostatistical modeling of rock fracture surface and simulation of shear tests

A.Marache
CDGA-Université Bordeaux I, Av. des Facultés, 33405 Talence Cedex, France
Laboratoire MSS-Mat, UMR 8579, Ecole Centrale Paris, Grande Voie des Vignes, 92295 Châtenay-Malabry Cedex, France

J.Riss
CDGA-Université Bordeaux I, Av. des Facultés, 33405 Talence Cedex, France

S.Gentier & J.-P.Chilès
BRGM, Direction de la Recherche, BP 6009, 45060 Orléans, France

ABSTRACT: To understand the hydromechanical behavior of jointed rock masses, the study of isolated rock joints is a key element. Nowadays many scientists stand for taking joints' morphology into account. In order to get numerical model for these joints, we propose an original method based on the use of the geostatistical tools. Using them allows to analyze the spatial relations between elevations (sampled from the joint), and their first and second derivatives. Next we present a method for the reconstruction of a fracture surface by using a variogram model derived from data coming from two different samples located on the same fracture a few centimeters apart. The method of reconstruction is performed in several steps in order to have a more and more accurate reconstruction. Finally, after the validation of the reconstructions by different ways, we show the implications of the size of digitalization of the fracture surfaces and of the kinds of reconstruction on the results of simulation of shear tests.

1 INTRODUCTION

The knowledge of the hydromechanical behavior of jointed rock masses is today very important in a lot of environmental problems (waste storage, rock mass stability, high enthalpy geothermal reservoirs, etc.). The study of jointed rock masses requires the study of isolated rock joints. It is well known that the morphology, the roughness of a joint is a key element for the understanding of its hydromechanical behavior. The aim of this paper is to show how very accurate numerical models of fracture surfaces can be inferred from quite unusual geostatistical methods and then successfully used in mechanical modeling.

2 PRESENTATION OF DATA

Fractures can be envisioned as two rough surfaces or walls in partial contact. The studied samples, denoted I and II, were cored trough a natural granitic fracture (Guéret, France). Sample I is a cylinder and the fracture is located at the middle of this cylinder, quite perpendicular to its axis. The diameter of the cylindrical sample is equal to 90 mm. Profiles of elevations have been recorded on the two walls of this sample (sampling step u = 0.5 mm) in four directions (a, b, c, d). Results presented in the following sections are those obtained by working on the lower wall (the same work was done for the upper wall; results for both walls are very closed). The recorded profiles on the lower wall have allowed to create a data base of 4096 co-ordinates {x,y,z} (Flamand 2000). Figure 1 shows the experimental recorded profiles in the four directions.

Profiles have been recorded along sample II with a smaller sampling step (u = 0.02 mm). The two samples are distant from a few centimeters and the axis of the two cylindrical samples are parallel one to the other. For this second sample, profiles are recorded along radii of the cylindrical sample and not in any preferential direction.

The aim is to characterize the most accurately as possible the morphology of sample I (because this

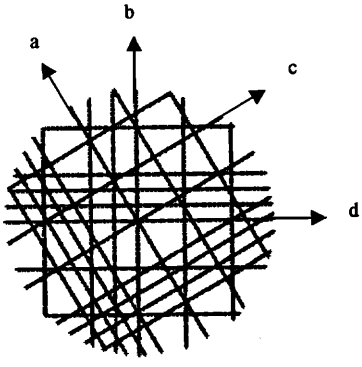

Figure 1. The four directions and the experimental profiles on the lower wall of sample I.

sample has been used for mechanical tests) and to obtain reconstructions of this sample (knowledge of elevations at each node of a grid). Sample II is only used to increase the accuracy while modeling sample I. In order to do that, we use the geostatistical tools.

3 GEOSTATISTICAL STUDY

3.1 *Experimental variograms*

In geostatistics, the variogram allows to characterize the possible spatial relations existing between sampled data. Here these data are the elevations and their first and second derivatives. The experimental variogram of any variable z is computed as follows (Armstrong 1998):

$$\gamma(h) = \frac{1}{2n}\sum_{i=1}^{n}\left(z_{x_i+h} - z_{x_i}\right)^2 \qquad (1)$$

The analysis of experimental variograms is here leaded on the sample I's lower wall.

Figure 2 shows the experimental directional variograms of elevations computed in the four directions.

Except for the b direction, variograms increase continuously when h increases. This is the proof that there is a trend in the data, the mean elevation is space-varying. This drift is observable on profiles recorded in the d direction. This drift masks all details in the spatial structure of elevations. Because the drift appears as linear on experimental profiles, we assume the drift to be planar in three dimensions.

So we work on the residual values z_r computed as shown equation 2:

$$z_r(x,y) = z(x,y) - (ax + by + c) \qquad (2)$$

with: z experimental elevations at any point (x,y) and (ax + by + c) the value of the planar drift.

All the following work will be done with the residual values $z_r(x,y)$ but at the end of the geostatistical work, the drift will be added in order to get z(x,y) values from which the numerical representation of the fracture surface is inferred.

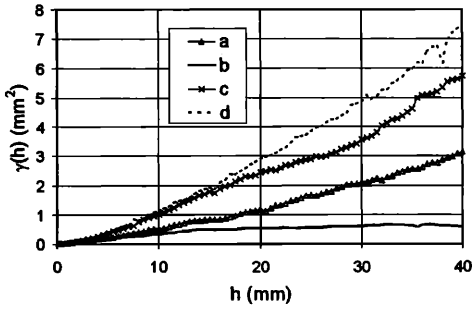

Figure 2. Experimental variograms of elevations in the four directions (sample I, lower wall).

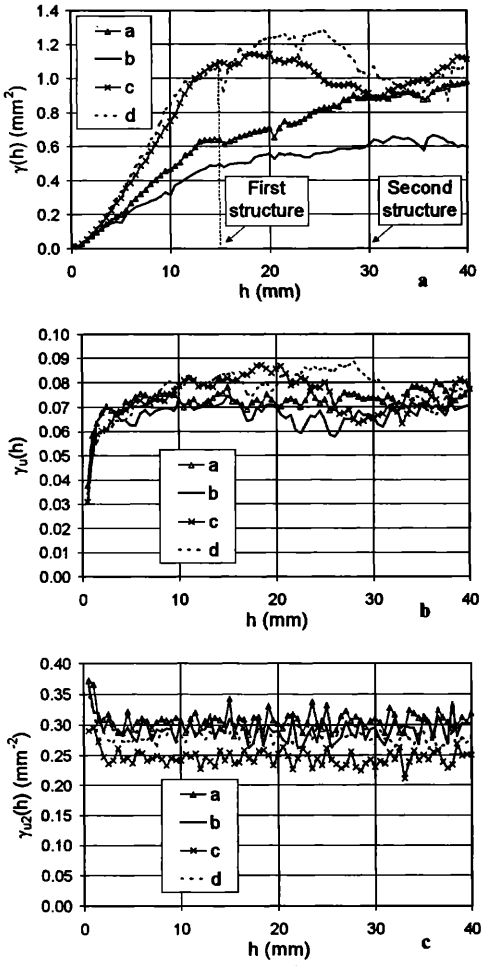

Figure 3. Experimental variograms of residual values (γ(h)) (a) and their first ($\gamma_u(h)$) (b) and second ($\gamma_{u2}(h)$) (c) derivatives (sample I).

Figure 3 shows the experimental directional variograms of the residuals γ(h) and those of their first $\gamma_u(h)$ and second $\gamma_{u2}(h)$ derivatives (sample I, recorded step u = 0.5 mm) in the four directions.

Figure 3 shows first a zonal anisotropy since the sills (value of γ(h) for the range) of the variograms vary with the direction, next it shows that the range (for values h greater than the range, variables are uncorrelated) of a first structure is equal to h = 15 mm whatever the direction is. Furthermore, in the c and d directions, a second structure appears for h = 30 mm.

On the variograms of first and second derivatives, the ranges of the observed structures are smaller than previously (ranges equal to 8 mm for the first derivatives and to 2 mm for the second derivatives); furthermore, the higher is the order of the derivative and the less obvious is the anisotropy.

The aim of the next section is to find a model that meets the previous observations.

3.2 *Variogram modeling*

Variogram modeling consists in finding an anisotropic model, which should be the sum of nested theoretical models. It should be noticed here that the model needs only to be fitted to the beginning of experimental variograms (see section 3.3). Furthermore, good variogram modeling can be obtained when the model is chosen so as to produce a good fit to the experimental variograms of residuals and to those of first and second derivatives, since the theoretical variograms of first and second derivatives of a given variable are available (Chilès & Gentier 1992, Marache et al., in prep.).

A model based on the only previous data could be derived but we decide to search a model based on data from both samples (I and II). With the use of sample II, we get more experimental variograms, so the model should be better constrained. Furthermore, elevations of sample II having been recorded with a smaller step (u = 0.02 mm) than those of sample I, this sample can allow to improve the quality of the model for small h values.

Because profiles of sample II have been recorded along radii without preferential direction, the computed variogram of residuals is an omnidirectional variogram.

The comparative analysis of variograms of samples I and II shows first, that the omnidirectional variogram of residual values of sample II (Fig. 4d) shows higher values than those observed for the directional variograms of sample I (Fig. 4a) and next, that values of the variogram of first derivatives of sample II are again higher than those of sample I. The first note is the consequence of a greater variability of data recorded on sample II than for sample I. The second point emphasizes that the variogram of first derivatives is dependant to the calculus step: the smaller is the step and the higher are the variogram values (Marache et al., in prep.).

However, a detailed analyze of the variograms of residuals values shows that the variogram values of sample II and the average variogram values of the b and d directions of sample I (main directions) are proportional (ratio = 5.1): that is this structural link existing between the two samples that we want to use in the modeling.

In order to do that, the variogram model will be chosen so as to fit well both to the experimental variograms of sample I (residual values, first and second derivatives), and sample II (residual values and first derivatives).

The chosen model is the sum of five nested elementary models (spherical, two Cauchy and two cubic); Figure 4a, b and c show the fitting for sample I and d and e for sample II; in the latest case the model is multiplied by the ratio 5.1. The number between parentheses on variograms of derivatives indicates the step for the computation of the derivatives.

The variogram model having been found, the next step in the geostatistical study is the reconstruction of the fracture surfaces.

3.3 *Reconstruction of the fracture surfaces*

The aim of the reconstruction of the fracture surfaces is to obtain a knowledge of residual values at each node of a pre-defined grid. Recall that, in order to get the final elevations (z(x,y)), the drift as defined in section 3.1 will be added at the end. The reconstruction is done on sample I. In order to estimate a residual value at a node, we use data located in a circular neighborhood of 8 mm from the point to be estimated (that's why we fit better for small h values than for high ones). The estimation is done by using either kriging or conditional simulation method. Kriging is the best method of estimation because it minimizes the error, but it smoothes results. Conditional simulation allows to introduce variability. The kriging estimator is an exact interpolator (the mean error is equal to zero), but kriging estimates are less dispersed than the true data; in order to avoid this phenomenon we use also conditional simulation that are useful to obtain realistic pictures of spatial variability (Chilès & Delfiner 1999).

The reconstruction is here performed in successive steps (two or three). At first , we filter the whole experimental set of data in order to keep only one point every 2 mm. We realize a first reconstruction with this filtered set of data in order to have a residual value at each node of a grid with a mesh of 2 mm square. The next step consists in combining the previously estimated values with the totality of the experimental data; the result is the set of residual estimated values at each node of a 0.5 mm grid mesh size. This result can be either the final result or another intermediate result; if so, we perform a last reconstruction to have a result with a mesh of 0.1 mm. At each step we can use either kriging or conditional simulation method. So we have a lot of possibilities and we obtain various results with a grid mesh either equal to 0.5 mm or to 0.1 mm. Figure 5 shows an example of reconstruction performed by kriging.

Since various numerical models (reconstructions) are available they must be checked against the background of our purpose: good quality of the numerical representation and its utility for simulations of mechanical tests. That's why it is now necessary to validate the various kinds of reconstruction in order to choose what are the best reconstructions which will be used later when simulating mechanical tests for rock joints.

3.4 *Validation of the reconstructions*

Various methods of validation are possible and we present here two distinct methods. First, the validation of the previous reconstructions is done by comparing experimental variograms and those computed with data resulting from the reconstructions. Next, the validation is done by comparing experimental

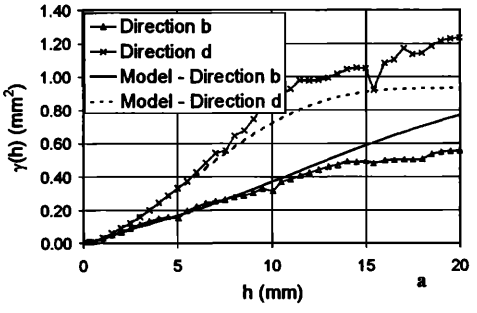

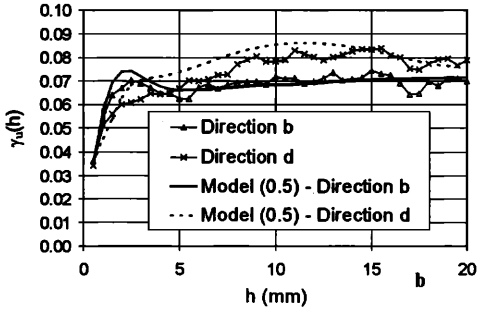

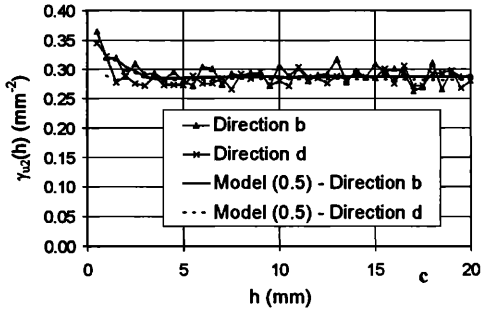

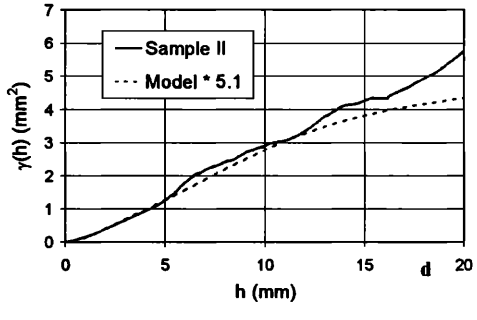

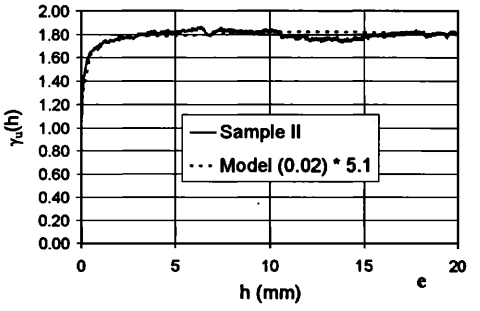

Figure 4. Variogram model. a, b and c: variograms of residual values, first and second derivatives of sample I; d and e: variograms of residual values and first derivatives of sample II.

and inferred distributions of morphological parameters such as colatitudes 2D (angularity of elements along profiles) (Marache et al. 2000) or radii of curvature. Radii of curvature are computed from a polynomial approximation realized on three successive points in a given direction.

Figure 6a shows the experimental variogram of first derivatives and those computed from a kriging and from a conditional simulation reconstruction. Figure 6b shows the experimental and inferred cumulative distributions of radii of curvature. These results are shown for the d direction, but conclusions are the same for all directions.

The same kind of conclusions can be drawn from the two methods of validations: in both cases kriging method smoothes the results and those from conditional simulation are in good agreement with the experimental data. In fact, we can observe for the kriging method lower values on variograms, so a lower variability of first derivatives than the experimental one. On the distribution of the radii of curvature, we observe higher values of radii of curvature for a given cumulative frequency than those observed on experimental results. The higher is a radius of curvature of an element and the more flattened is this element, so this is again a proof of the smoothing resulting from the kriging method. Results obtained from conditional simulation are in both cases in good agreement with experimental results.

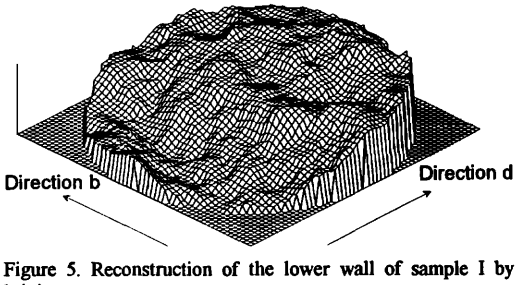

Figure 5. Reconstruction of the lower wall of sample I by kriging.

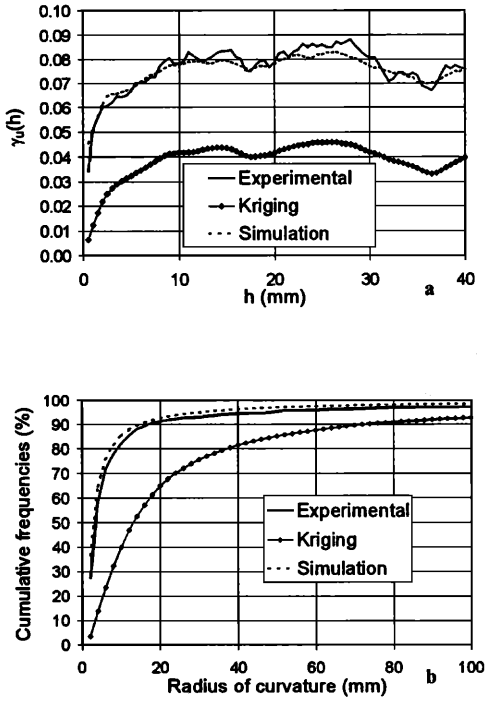

Figure 6. Validations of the reconstructions. a: variograms of first derivatives; b: radii of curvature.

Since kriging smoothes results, a part of the roughness on the fracture surface is removed. As a contrary, conditional simulation gives, at the recorded step, a variability of the angularity of the fracture and of its curve statistically identical to the real fracture. So the choice of the reconstruction for simulations of mechanical tests will depend of what we need. If we study micromechanical deformations, conditional simulation will be preferred because of a bigger variability in the morphology; if we study the shearing behavior for great tangential displacements, kriging or conditional simulation will give same results.

4 SIMULATION OF SHEAR TESTS

A computer code has been developed in order to study the mechanical behavior of rock joints under normal (Hopkins 1990) and shear stresses (Marache et al. 2001). It should be noticed that we focus our attention on the elastic phase of the shear test with constant normal load, before the apparition of damage (breaking or crushing). As a consequence the first step of the simulation is the simulation of a normal loading. The simulation of the normal loading allows to determine what are the contact points between the two rough surfaces before the beginning of the shear test. Validations of these simulations are available in Hopkins (1990) and Marache et al. (2001).

For the simulations of the tests, we need to know elevations at each point of a grid for the two walls, what was available for the lower wall from the previous geostatistical work. In order to obtain the reconstruction of the upper wall, two solutions are possible:

– either we use a geostatistical reconstruction of the upper wall (as previously for the lower wall).

– or we use a cast of the void space located between the two walls, so as to know the void aperture at each node of the same grid than for the reconstruction of the fracture surface of the lower wall (Gentier et al. 1996). To obtain the upper wall, we can add at each node of the grid the void aperture to the elevation of the lower wall.

We present in this paper results based on the second method.

For the simulations of the tests, on sample I, the Young's modulus of the rock will be equal to 30,853 MPa and the Poisson's ratio to 0.19.

4.1 *Influence of the grid size*

The aim of this part is to find the best size for the grid mesh (0.5 mm, 1 mm, 1.5 mm or 2 mm) in order to combine accuracy (the finer is the mesh size and the more accurate are the results) and time of computation (the finer is the mesh size and the longer is the time of computation). Note that for the moment, even if reconstructions with a grid mesh equal to 0.1 mm are available, they can't be used because of the too big number of points for which we know an elevation.

The aim of the model is to predict the closure of the fracture as a function of the normal load which is applied on it. The result of the normal loading is the normal stress applied as a function of the vertical displacement (closure of the fracture). Figure 7 shows the results of the normal loading simulation with the four different sizes of grid mesh.

When the grid mesh size decreases, the closure of the fracture is less important (for a same normal stress, the greater is the mesh size, the smaller is the vertical displacement) and the stiffness is slightly smaller. However, one can see a quick convergence of the graphs obtained for grid mesh sizes equal to 1 m and 0.5 mm. In all cases, the slope of the graph for great vertical displacements is the same, so the behavior of the fracture is the same for a high proportion of contact area whatever the grid mesh size is. Results shown on Figure 7 are representative of the majority of realized simulations. In order to realize more simulations, we have worked also on a part of the whole fracture surface. By analyzing results of all simulations, results for the grid meshes

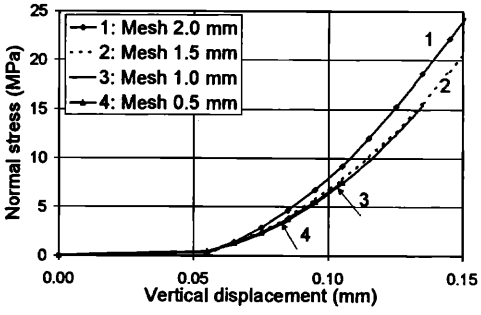

Figure 7. Influence of the grid size on the normal loading simulation.

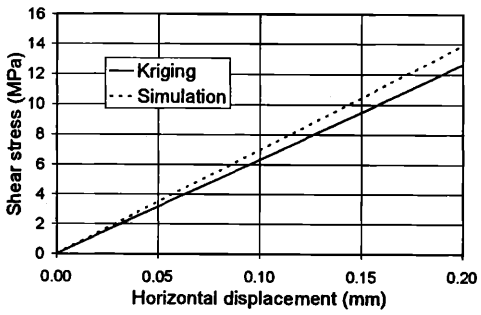

Figure 8. Influence of the kind of reconstruction on the shear loading.

1.5 mm and 1 mm are sometimes more different than those observed on Figure 7, but results for the grid meshes 1 mm and 0.5 mm are always very similar. Because results obtained with step 1 mm and 0.5 mm are quite closed, and because time of computation is shorter for the 1 mm case, we can take reconstructions done at 1 mm of grid mesh size for future works without big errors.

4.2 *Influence of the kind of reconstruction*

4.2.1 *Normal loading*

In the model we use, it is assumed that a joint can be modeled by two parallel half-spaces separated by variable height asperities so we need only to know the geometry of the void space. Given we have chosen to work with the cast of the void space, it is obvious that the kind of reconstruction has no influence while simulating normal loading.

4.2.2 *Shear loading*

In this section simulations are computed using numerical representation of the fracture surface on a grid with a mesh size equal to 1 mm.

Simulations are realized for a constant normal stress equal to 7 MPa. Results of the shear loading are given as applied tangential stress function of the horizontal displacement. Since we assume that we are in the elastic behavior stage and that the number of contact points doesn't change during this phase, the tangential stress increases linearly as a function of the horizontal displacement. Figure 8 shows results from reconstructions obtained with kriging and with conditional simulation.

One can see on Figure 8 that the obtained tangential stiffness (slope of the straight line defined by the shear stress as a function of the horizontal displacement) is greater for the result obtained from the conditional simulation reconstruction. In the developed code, in order to take the morphology of rock joints surfaces into account, we use the angularity (θ_2) of elements in the direction of shearing as defined Figure 9.

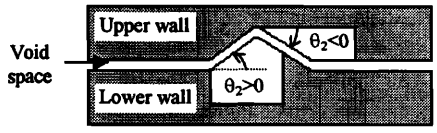

Figure 9. Angularity associated to the elements in the shear process.

The greater is the angle θ_2 of an element and the more important is the force required to perform a given displacement. We have shown in section 3.4 that the reconstructions performed by kriging, although of good quality, show a smoothing of the values, smoothing more accentuated when we look the derivatives. As a contrary, conditional simulation allows to introduce variability (see section 3.4). So values of angularity are usually greater with conditional simulation reconstructions. That's why the tangential stiffness is greater when we use the reconstructions obtained by conditional simulation.

5 CONCLUSIONS AND PERSPECTIVES

Understanding the hydromechanical behavior of rock joints under normal and shear stresses requires a accurate knowledge of their morphology. We have shown in this paper the power of the geostatistical tool in order to characterize this morphology and to reconstruct fracture surfaces. Furthermore, we have shown how to obtain results for a sample by combining data providing from two neighboring samples. This method allows to obtain different reconstructions, all validated by various ways, and to know what are the best reconstructions as a function of what we need from a mechanical point of view.

Simulations of normal and shear tests have allowed to select what are the best size of reconstructions in order to combine accuracy and time of computation. Furthermore, they have shown the implications of the geostatistical work on the results of simulations.

The aim is now to improve and to continue the

development of the mechanical model of the shear test in order to simulate a complete test up to 5 mm of horizontal displacement, by taking dilatancy and damage into account, and to continue to analyze the differences between reconstructions used.

REFERENCES

Armstrong, M. 1998. *Basic linear geostatistics.* Springer.

Chilès, J.-P. & Delfiner, P. 1999. *Geostatistics – Modeling spatial uncertainty.* Wiley-Interscience Publication.

Chilès, J.-P. & Gentier, S. 1992. Geostatistical modelling of a single fracture. *Geostatistics Troia'92, International Congress for Geostatistics*, 1: 95-108.

Flamand, R. 2000. *Validation d'une loi de comportement mécanique pour les fractures rocheuses en cisaillement.* PhD of the University of Québec at Chicoutimi - Specialty Mineral resources.

Gentier, S., Billaux, D., Hopkins, D.L., Davias, F. & Riss, J. 1996. Images and modeling of the hydromechanical behavior of a fracture. *Microsc. Microanal. Microstruct.* 7: 513-519.

Hopkins, D.L. 1990. *The effect of surface roughness on joint stiffness, aperture, and acoustic wave propagation.* PhD of the University of California at Berkeley, Specialty Engineering, Materials Science and Mineral Engineering.

Marache, A., Hopkins, D.L., Riss, J. & Gentier, S. 2001. Influence of the variation of mechanical parameters on results of the simulation of shear tests on a rock joint. *Eurock 2001, Espoo, 3-7 June 2001.*

Marache, A., Riss, J., Gentier, S. & Chilès, J.-P. Method of characterisation and reconstruction of a rock fracture surface by geostatistics. In prep.

Marache, A., Riss, J., Lopez, P. & Gentier, S. 2000. Geostatistical modelling of a fracture surface: implication in shear simulation by image analysis. *STERMAT 2000, Cracovie, 20-23 September 2000*, 265-271.